Available online at www.sciencedirect.com
SCIENCE DIRECT
Journal of Magnetic Resonance 181 (2006) 316–326
JMR Journal of Magnetic Resonance
www.elsevier.com/locate/jmr

# Multi-dimensional $^{1}H$–$^{13}C$ HETCOR and FSLG-HETCOR NMR study of sphingomyelin bilayers containing cholesterol in the gel and liquid crystalline states

Gregory P. Holland [1], Todd M. Alam *

*Department of Electronic and Nanostructured Materials, Sandia National Laboratories, Albuquerque, NM 87185-0886, USA*

Received 17 March 2006; revised 23 May 2006
Available online 22 June 2006

**Abstract**

$^{13}C$ cross polarization magic angle spinning (CP-MAS) and $^{1}H$ MAS NMR spectra were collected on egg sphingomyelin (SM) bilayers containing cholesterol above and below the liquid crystalline phase transition temperature ($T_m$). Two-dimensional (2D) dipolar heteronuclear correlation (HETCOR) spectra were obtained on SM bilayers in the liquid crystalline ($L_\alpha$) state for the first time and display improved resolution and chemical shift dispersion compared to the individual $^{1}H$ and $^{13}C$ spectra and significantly aid in spectral assignment. In the gel ($L_\beta$) state, the $^{1}H$ dimension suffers from line broadening due to the $^{1}H$–$^{1}H$ homonuclear dipolar coupling that is not completely averaged by the combination of lipid mobility and MAS. This line broadening is significantly suppressed by implementing frequency switched Lee–Goldburg (FSLG) homonuclear $^{1}H$ decoupling during the evolution period. In the liquid crystalline ($L_\alpha$) phase, no improvement in line width is observed when FSLG is employed. All of the observed resonances are assignable to cholesterol and SM environments. This study demonstrates the ability to obtain 2D heteronuclear correlation experiments in the gel state for biomembranes, expands on previous SM assignments, and presents a comprehensive $^{1}H/^{13}C$ NMR assignment of SM bilayers containing cholesterol. Comparisons are made to a previous report on cholesterol chemical shifts in dimyristoylphosphatidylcholine (DMPC) bilayers. A number of similarities and some differences are observed and discussed.


*Keywords:* 2D HETCOR; FSLG; Sphingomyelin; Cholesterol; Liquid ordered phase; Membranes; Gel phase; Lipid

## 1. Introduction

The viewpoint that cellular membranes exist in a continuous liquid crystalline ($L_\alpha$) phase is rapidly changing. Recent studies strongly suggest that the presence of cholesterol can cause lipids with high $L_\alpha$ phase transition temperatures ($T_m$), to form liquid ordered ($l_o$) phases in biological membranes [1,2]. The $l_o$ phase differs from the $L_\alpha$ liquid crystalline phase in that it exhibits a higher degree of acyl chain order [3]. It has been shown in a number of model ternary systems that these $l_o$ phases, rich in cholesterol and high $T_m$ saturated chain lipids, will phase separate in the presence of low $T_m$ unsaturated lipids [4–11]. Sphingomyelin (SM) is one of the primary saturated lipids that comprise mammalian cells [12] and has been indicated in the formation of $l_o$ domains or rafts in cellular membranes [1,2,13,14]. These raft domains are postulated to be involved in a number of vital cellular processes such as endocytosis and cell signaling [13], protein sorting [15] and cholesterol shuttling [16]. Convincing evidence exists that cholesterol prefers to pack with saturated lipids over unsaturated lipids and further, that cholesterol favors sphingolipids over glycerophospholipids [17]. Although surmounting evidence supports the existence of cholesterol rich $l_o$ domains of SM in cellular and model membranes systems, the specific molecular contacts that mediate this sphingolipid–cholesterol interaction are still

* Corresponding author. Fax: +1 505 844 9324.
*E-mail address:* tmalam@sandia.gov (T.M. Alam).
[1] Present address: Magnetic Resonance Research Center, Department of Chemistry and Biochemistry, Arizona State University, Tempe, AZ 85287-1604, USA.

1090-7807/$ - see front matter © 2006 Elsevier Inc. All rights reserved.
doi:10.1016/j.jmr.2006.05.017

far from understood. In order to obtain a comprehensive understanding of the structure–function role of lipid rafts in cell membranes a more thorough understanding of these molecular interactions is needed.

$^{1}$H magic angle spinning (MAS) and $^{13}$C cross-polarization (CP-)MAS NMR spectroscopy are powerful tools for studying molecular level structure and dynamics in multilamellar vesicles (MLV's) and have been implemented in the lipid community for decades. A significant number of $^{1}$H and $^{13}$C NMR studies regarding the interaction of cholesterol in glycerophospholipid bilayers have appeared [18–25]. Significantly fewer NMR studies have appeared on SM [26,27] and SM/Chol [28–30] bilayer systems. All of these studies focus primarily on the $L_\alpha$ phase due to the improved resolution observed compared to the $L_\beta$ gel phase particularly, in $^{1}$H MAS NMR spectra [20].

Most of the $^{1}$H and $^{13}$C NMR studies of lipid membranes that have appeared in the literature on MLV's are one-dimensional (1D) studies, although some two-dimensional (2D) $^{1}$H NOESY [31–33], $^{1}$H/$^{31}$P heteronuclear correlation (HETCOR) [34], and $^{1}$H/$^{13}$C HETCOR [35,36] studies have emerged. More recently 2D studies involving cholesterol containing dimyristoylphosphatidylcholine (DMPC) bilayers have also appeared [37–39]. Similar to the majority of the 1D studies all these 2D studies have been limited solely to the $L_\alpha$ phase (above $T_m$). A better understanding of lipid cholesterol organization and sterol–lipid interactions will come from going to multi-dimensional experiments below $T_m$ where dipolar interactions are stronger (due to reduced molecular motions) and contacts between the lipid and cholesterol can potentially be detected. In the present study, $^{1}$H MAS and $^{13}$C CP-MAS NMR spectra are obtained for pure SM bilayers and those containing cholesterol above and below $T_m$. Conventional 2D dipolar $^{1}$H/$^{13}$C HETCOR on SM yield high resolution spectra above $T_m$, while below $T_m$ high resolution type spectra are only observed when frequency switched Lee–Goldburg (FSLG) $^{1}$H homonuclear decoupling is implemented during the evolution period [40–44]. The isotropic chemical shifts of SM and cholesterol incorporated in SM bilayers are reported and comparisons are made to the chemical shifts observed for cholesterol in DMPC bilayers [37].

## 2. Experimental

### 2.1. Materials

Egg sphingomyelin (SM) and cholesterol (Chol) were purchased from Avanti Polar Lipids (Alabaster, AL) and used as received. The SM had the following acyl chain composition: 84% 16:0, 6% 18:0, 2% 20:0, 4% 22:0, 4% 24:0 and contained no unsaturated acyl chains.

### 2.2. Sample preparation

Pure lipid samples were prepared by mixing the lipid with de-ionized water or $D_2O$ in a conical vial with a vortex mixer. This was followed by a minimum of 5 freeze–thaw cycles in dry ice and a warm water bath set to 60 °C (above $T_m$ for SM). Buffer was not used in any of the lipid mixtures. Samples containing cholesterol were first combined and dissolved in chloroform followed by vacuum drying overnight to remove the solvent. The samples were then hydrated with the above procedure. The samples are MLV's greater than 1 μm in diameter as confirmed by $^{31}$P static NMR (data not shown). All lipid samples were 33 wt% phospholipid (67 wt% $H_2O$). The binary cholesterol-containing sample was 33 mol % cholesterol. The lipid samples were transferred to 4 mm zirconia MAS rotors and sealed with kel-F inserts and caps. The typical volume of MLV sample for NMR analysis was 50–100 μL corresponding to 25–50 mg of phospholipid. The samples were stored in a −20 °C freezer when NMR experiments were not being performed.

### 2.3. NMR spectroscopy

$^{1}$H MAS and $^{13}$C CP-MAS NMR spectra were collected on a Bruker Avance 400 spectrometer equipped with a 4 mm broadband double resonance MAS probe. The MAS speed ($\nu_R$) was set to 10 kHz and controlled to ±1 Hz in all MAS experiments with a Bruker MAS control unit. The $^{1}$H spectra were collected with a 2.5 μs π/2 and a 10 s recycle delay. The $^{1}$H spectra were referenced to TMS ($\delta = 0$) by setting the SM methyl resonance (H16′, H18) to 0.9 ppm [26]. The 1D $^{13}$C CP-MAS experiments utilized a 4 μs $^{1}$H π/2 and a 2 ms contact time. The 1D CP pulse sequence implemented a ramped (50 → 100%) spin-lock pulse on the $^{1}$H channel and a square contact pulse on the $^{13}$C channel [45]. 2D dipolar HETCOR experiments were performed to correlate $^{13}$C and $^{1}$H chemical shifts. This experiment is analogous to the wideline separation (WISE) experiment previously described by Schmidt-Rohr et al. with the exception that it is performed at a higher MAS speed [46]. These increased MAS speeds are known to enhance the resolution in the $^{1}$H dimension [47]. HETCOR experiments with Lee–Goldburg (LG) $^{1}$H homonuclear decoupling [40] were performed as previously described [41–44,48] where FSLG decoupling is applied during the $t_1$ evolution period. The LG $^{1}$H homonuclear decoupling implemented in these experiments is analogous to the flip-flop LG (FFLG) previously described by Mehring and Waugh where a frequency shift was utilized to achieve an effective field along the magic angle [49]. In the FSLG HETCOR experiment a LG-CP condition was used for $^{1}$H → $^{13}$C polarization transfer. The $^{1}$H dimension required the theoretical scaling factor $\cos\theta = 1/\sqrt{3}$ in the FSLG-HETCOR spectra [41]. A moderate power $^{1}$H two pulse phase modulation (TPPM) decoupling field strength of 62.5 kHz was implemented during acquisition of the free induction decay in all $^{13}$C detected experiments using a 15° phase shift [50]. The FSLG homonuclear decoupling field strength was also 62.5 kHz. The pulse sequences for dipolar HETCOR and FSLG-HETCOR are depicted in Fig. 1.

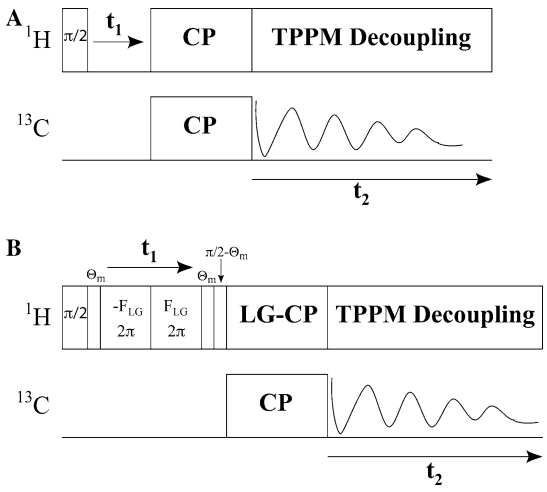


Fig. 1. 2D NMR pulse sequences for (A) $^1$H/$^{13}$C dipolar HETCOR with CP polarization transfer and TPPM decoupling and (B) FSLG-HETCOR with LG-CP polarization transfer and TPPM decoupling (B).

Typical acquisition parameters for 2D experiments were 256 or 512 scan averages and 64 or 128 $t_1$ points. A recycle delay of 5 and 2 s was utilized in the 1D and 2D $^{13}$C detected experiments, respectively. The isotropic $^{13}$C chemical shift was set using a secondary reference of solid glycine (carbonyl $\delta = 176.03$ ppm with respect to TMS $\delta = 0$ ppm). The temperature was controlled to $\pm 0.2$ K with a Bruker VT unit. The actual sample temperature does not correlate with the set sample temperature due to heating effects caused by MAS and decoupling, which can be significant. The actual sample temperature was calibrated as described previously where the chemical shift of the $^1$H water resonance in the lipid sample is monitored under MAS and decoupling conditions [51]. The heating effect of MAS at 10 kHz and $^1$H decoupling at 62.5 kHz for ~30 ms was found to be 7 and 9 °C, respectively. These heating effects are accounted for in all experiments reported in this paper. These heating effects can result in modest membrane dehydration that can be ignored for most applications [52].

Assignments of SM resonances were based on previous sphingolipid NMR studies [26,53]. Some additional assignments not made previously could be made by examining the 2D HETCOR spectra. The cholesterol resonances observed in SM bilayer samples were assigned based off a previous study on cholesterol in DMPC bilayers [37]. The full width at half maximum (FWHM) or line width was extracted by fitting the resonances in the DMFIT software package [54]. The structure of SM and cholesterol are depicted in Fig. 2 with the nomenclature.

## 3. Results and discussion

### 3.1. One-dimensional $^1$H MAS NMR of SM bilayers containing cholesterol

The $^1$H MAS NMR spectra of SM and SM/Chol samples collected at 325 K are displayed in Fig. 3. This temperature is above $T_m$ (~40 °C) hence, SM is in the $L_\alpha$ liquid crystalline phase [55]. Both the SM/Chol (A) and the pure SM sample (B) display sharp resonances that can be assigned to SM protons (see Table 1) based on previous $^1$H MAS NMR studies on SM bilayers [26]. Narrow $^1$H line widths are observed in the $L_\alpha$ phase compared to the line widths expected in a rigid organic solid. These narrower line widths can be attributed to rapid lipid lateral diffusion, fast axial rotation about the bilayer normal, and *trans/gauche* isomerizations that significantly reduce the inter- and intramolecular $^1$H–$^1$H dipole–dipole interactions [20,22,23]. The line widths of the cholesterol containing sample are slightly broader, FWHM = 60 Hz for SM/Chol compared to 46 Hz for SM measured at the $(CH_2)_n$ resonance. The slightly broader line widths in the cholesterol-containing sample can be attributed to a more restricted mobility of the saturated lipid chain caused by packing with cholesterol. This hinders some of the axial rotation and *trans/gauche* isomerizations that average the $^1$H dipole–dipole interactions. This is consistent with previous $^2$H static NMR studies on phospholipid/cholesterol

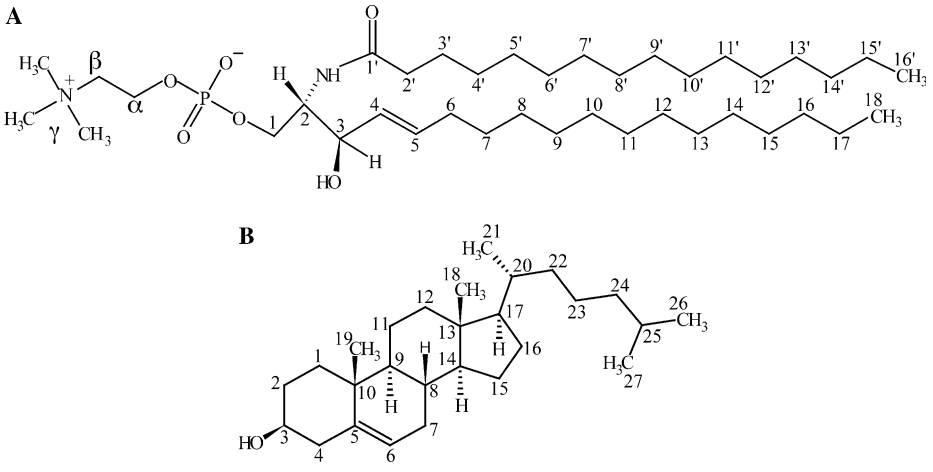


Fig. 2. The structure of (A) the primary component of egg SM and (B) cholesterol with the numbering nomenclature.

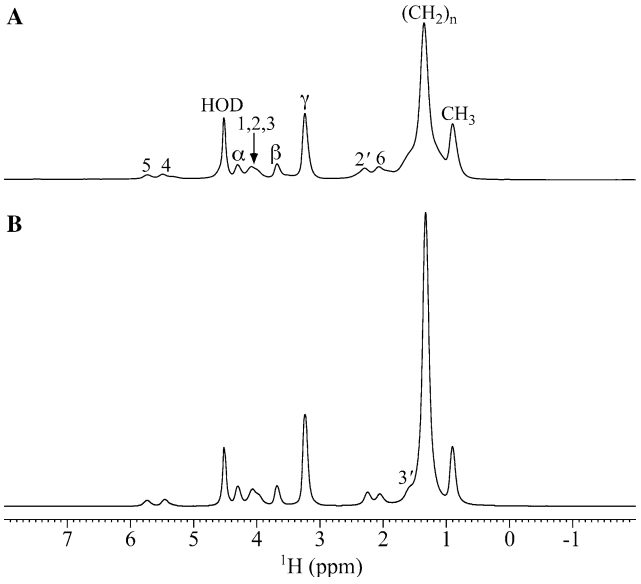


Fig. 3. $^1$H MAS NMR spectrum collected at $\nu_R = 10$ kHz and 325 K (above $T_m$) for (A) SM/Chol and (B) pure SM bilayers.

Table 1
$^1$H chemical shifts in ppm of SM extracted from MAS NMR spectrum collected at 325 K (above the $T_m$ of SM)

| Assignment | SM $L_\alpha$ phase |
|---|---|
| H18/H16′ | 0.9 |
| $(CH_2)_n$ | 1.3 |
| H3′ | 1.6 |
| H6 | 2.1 |
| H2′ | 2.2 |
| Hγ | 3.2 |
| Hβ | 3.7 |
| H1,2,3 | 4.1 |
| Hα | 4.3 |
| H4 | 5.5 |
| H5 | 5.7 |

mixtures above $T_m$ where a larger $^2$H quadrupole splitting was observed when cholesterol was incorporated in the bilayer. This was attributed to a decrease in chain mobility with a higher probability of *trans* conformations [56–58]. Since the structural and dynamic characteristics of phospholipid/cholesterol mixtures with significant cholesterol contents ($\geqslant$25%) are intermediate between the $L_\beta$ gel and $L_\alpha$ liquid crystalline phase, they have been termed the $l_o$ phase [3,22,59]. A higher probability of *trans* conformations was also confirmed by monitoring the $^{13}$C chemical shift of the $(CH_2)_n$ resonance of SM in SM/Chol mixtures with $^{13}$C CP-MAS NMR (see below).

There are a few $^1$H resonances observed for SM in the present study that were not resolved in previous $^1$H MAS NMR spectra of SM bilayers. Particularly, the C4 and C5, C2′ and C6, and the high ppm shoulder of the main $(CH_2)_n$ resonance that can be assigned to C3′ [26]. The assignment of these peaks was assisted by 2D dipolar HETCOR spectra discussed below. The lower resolution in the latter study can be attributed to the lower spectrometer field and slower MAS speed utilized. It should also be noted that no specific cholesterol peaks are resolved in $^1$H MAS NMR spectra indicating a need for $^{13}$C-detected NMR experiments to increase chemical shift dispersion and detect cholesterol resonances. The reason for the lack of resolved cholesterol resonances in the $^1$H MAS NMR spectrum is attributed to the tight chemical shift range (0.5–2.5 ppm) and broad line widths.

The $^1$H MAS NMR spectra of SM and SM/Chol samples at 301 K are displayed in Fig. 4. At this temperature SM is below $T_m$ and exists in the $L_\beta$ gel state. Even at 10 kHz MAS the main acyl chain $^1$H resonance is broad (FWHM = 1.3 kHz), and only the $\alpha$, $\beta$, and $\gamma$ resonances of the headgroup are resolved. More rapid MAS speeds could not be pursued due to a centrifugal effect where the water begins to separate from the lipid. These types of problems can result in lipid dehydration and have been discussed previously [52,60]. The poor resolution observed in the $L_\beta$ phase is due to the $^1$H–$^1$H homonuclear dipolar coupling and has been discussed previously for phospholipids in the gel state [20]. The tight acyl chain packing and interdigitation in the $L_\beta$ gel phase results in a decrease in the chain mobility that dynamically averages the $^1$H homonuclear dipole–dipole coupling in the case of the $L_\alpha$ liquid crystalline phase discussed above. When cholesterol is incorporated in the bilayer the acyl chain packing and interdigitation is reduced and the fluidity of the bilayer is increased [61]. This results in a narrowing of the $^1$H line widths, specifically for the $(CH_2)_n$ resonance, where the FWHM = 1.3 kHz in the pure SM sample compared to 400 Hz for SM/Chol. This shows that when cholesterol is in contact with the saturated chains of SM it causes an increase in chain mobility and decrease in *trans* conformations below $T_m$. Thus, cholesterol has the opposite effect on SM above and below $T_m$. Above $T_m$ cholesterol presence

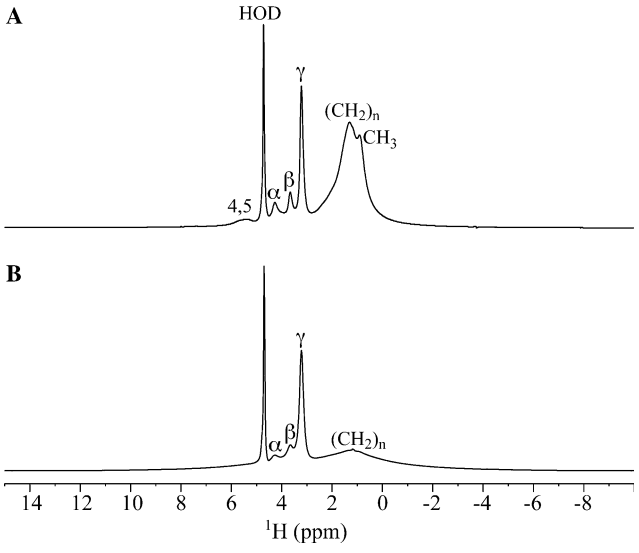


Fig. 4. $^1$H MAS NMR spectrum collected at $\nu_R = 10$ kHz and 301 K (below $T_m$) for (A) SM/Chol and (B) pure SM bilayers.

decreases chain mobility (increases order) and below $T_m$ it increases chain mobility (decreases order) compared to pure SM. This is consistent with previous interpretations from $^{13}C$ MAS NMR on SM/Chol and dipalmitoylphosphatidylcholine (DPPC)/Chol bilayers where the chemical shift of the $(CH_2)_n$ $^{13}C$ resonance is indicative of the amount of mobile *gauche* conformers present [21,23,28]. These results also agree with the early static $^1H$ NMR and ESR work of Olfield et al. on SM dispersions containing cholesterol [62,63].

### 3.2. One-dimensional $^{13}C$ CP-MAS NMR of SM bilayers containing cholesterol

The 1D $^{13}C$ CP-MAS NMR spectra of SM bilayers containing cholesterol at 310 K (below $T_m$) are displayed in Fig. 5. Numerous resonances are resolved that can be assigned to SM and cholesterol (see Tables 2 and 3). The subscript c denotes cholesterol resonances. The presence of cholesterol in the bilayer results in a sharpening of many of the SM $^{13}C$ resonances. This is particularly evident for C18/C16′, C17/C15′, $(CH_2)_n$, C3, and C3′ resonances, emphasizing the impact of cholesterol on the sphingosine backbone and saturated chain region of the lipid. The resonances of the acyl chain display chemical shifts to lower ppm in the cholesterol-containing sample. This can be attributed to an increase in *gauche* conformations as discussed previously in SM/Chol bilayers [28] and mentioned in the previous section with respect to the $^1H$ line width. The $(CH_2)_n$, C3′, C17/C15′resonances shift downfield 0.3, 0.3, and 0.5 ppm with incorporation of cholesterol, respectively. The larger shift observed for the C17/C15′ resonance could potentially indicate a greater degree of induced chain mobility and disorder towards the end of the saturated chain when cholesterol is present in SM below $T_m$. The headgroup resonances: $C_\gamma$, $C_\alpha$, and $C_\beta$ display consistent chemical shifts and line widths when cholesterol is present. However, a slight decrease in CP efficiency is observed for these resonances indicating a decrease in the C–H dipolar coupling. This is not surprising considering $^{31}P$ static NMR results on SM/Chol bilayers below $T_m$ showed that axial headgroup rotations were similar to that occurring in the $L_\alpha$ phase of SM [64]. It is likely that these headgroup motions, which average the $^{31}P$ chemical shift anisotropy, could potentially dynamically average the C–H coupling. An increase in mobility of the headgroup region is also consistent with the $^1H$ results where slightly sharper $^1H$ headgroup resonances were observed in SM/Chol sample compared to the pure SM sample. The carbonyl resonance, C1′, displays a 0.2 ppm shift downfield when cholesterol is present. This has been attributed to a change in the hydrogen bonding environment at the carbonyl site in previous studies on phospholipid/cholesterol mixtures [28,65]. It appears that a change in water hydrogen bonding is the more probable explanation for this shift rather than a direct hydrogen bond with the OH of cholesterol [28,30].

The $^{13}C$ CP-MAS spectra of SM and SM/Chol bilayers at 334 K (above $T_m$) are presented in Fig. 6. Comparison of the spectrum obtained for SM in the $L_\alpha$ phase (Figs. 6B and D) to the one obtained on the $L_\beta$ phase (Figs. 5B and D) reveals significantly sharper lines in the $L_\alpha$ phase. The acyl chain resonances: $(CH_2)_n$, C17/C15′, C3′, C6, and C16/C14′ sharpen substantially and large upfield shifts are observed between 1 and 2 ppm. Again, this is consistent with an increase in chain mobility and fraction of *gauche* conformers in the $L_\alpha$ phase compared to the primarily *trans* $L_\beta$ phase. Note, C16/C14′ and C6 are not well resolved in the $L_\beta$ phase of SM without cholesterol but, are clearly observed in the $L_\alpha$ phase due to the chemical shifts of the saturated acyl chain groups. These groups are assigned based on liquid state NMR sphingomyelin studies [53] and dipolar HETCOR experiments discussed below. The C4 and C5 double bond groups also display a significant sharpening in both SM and SM/Chol in comparison to the SM $L_\beta$ phase indicating an increased mobility at these sites as well.

When comparing the SM/Chol $^{13}C$ CP-MAS spectrum to the SM spectrum above $T_m$ some noticeable differences

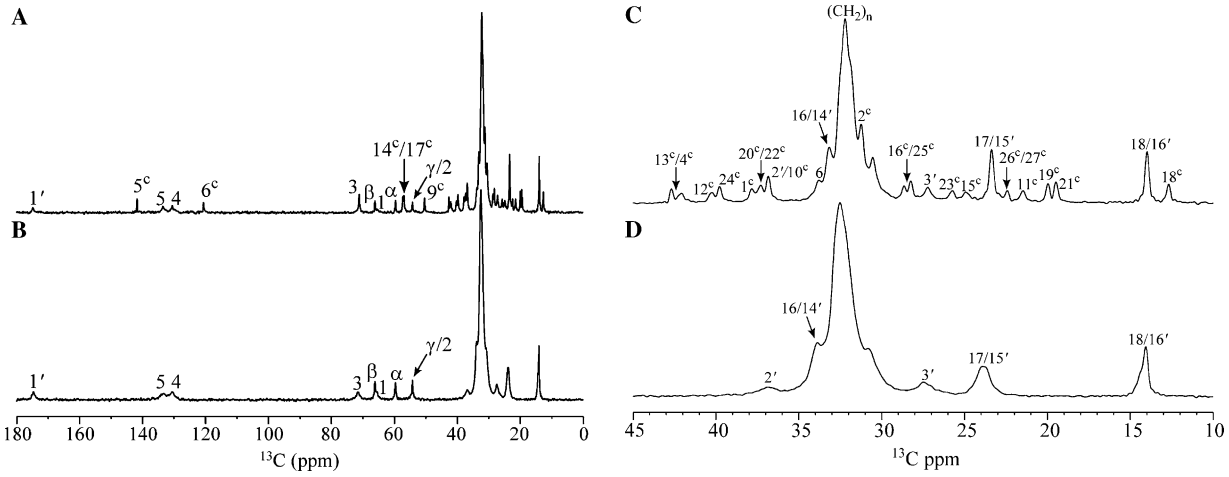


Fig. 5. $^{13}C$ CP-MAS NMR spectrum collected with a 2 ms contact time at 310 K (below $T_m$) for (A) SM/Chol and (B) pure SM bilayers. A blow up of the crowded acyl chain region (10–45 ppm) is shown for (C) SM/Chol and (D) SM. The superscript c denotes cholesterol resonances.

Table 2
$^{13}C$ chemical shifts in ppm of SM extracted from CP-MAS NMR spectra of pure SM and SM/Chol bilayers

| Assignment | SM $L_\beta$ phase | SM $L_\alpha$ phase | SM/Chol $l_o$ phase (310 K, below $T_m$) | SM/Chol $l_o$ phase (334 K, above $T_m$) |
|---|---|---|---|---|
| C18/C16′ | 14.1/14.4 | 13.8 | 14.0 | 13.9 |
| C17/C15′ | 23.9 | 22.8 | 23.4 | 23.0 |
| C3′ | 27.5 | 26.5 | 27.2 | 26.9 |
| $(CH_2)_n$[a] | 30.8 | 29.9 | 30.6 | 30.6 |
| $(CH_2)_n$[a] | 32.5 | 30.5 | 32.2 | 31.5 |
| C16/C14′ | 33.9 | 32.2 | 33.2 | 32.7 |
| C6 | [b] | 33.0 | 33.8 | 33.4 |
| C2′ | 36.9 | 36.6 | 36.9 | 36.8 |
| Cγ/C2 | 54.3 | 54.3 | 54.3 | 54.4 |
| Cα | 59.7 | 59.6 | 59.7 | 59.7 |
| C1 | 65.4 | 65.4 | 65.5 | 65.4 |
| Cβ | 66.2 | 66.3 | 66.2 | 66.3 |
| C3 | 71.6 | 71.3 | 71.2 | 71.2 |
| C4 | 130.6 | 130.3 | 130.5 | 130.4 |
| C5 | 133.2 | 133.9 | 133.5 | 133.7 |
| C1′ | 174.6 | 174.6 | 174.8 | 174.8 |

Spectra were obtained at 310 and 334 K (above and below the $T_m$ of SM).
[a] Acyl chain resonances including C4′–C13′/C7–C15.
[b] Not resolved in this phase.

Table 3
$^{13}C$ chemical shifts in ppm of cholesterol extracted from CP-MAS NMR spectra of SM/Chol bilayers

| Assignment | SM/Chol $l_o$ Phase (310 K, below $T_m$) | SM/Chol $l_o$ phase (334 K, above $T_m$) |
|---|---|---|
| C18 | 12.7 | 12.5 |
| C21 | 19.5 | 19.3 |
| C19 | 20.0 | 19.8 |
| C11 | 21.5 | 21.5 |
| C26/C27 | 22.4 | 22.4 |
| C15 | 24.9 | 24.9 |
| C23 | 25.7 | 25.3 |
| C25 | 28.3 | 28.1 |
| C16 | 28.7 | 28.6 |
| C2 | 31.3 | 30.6 |
| C7/C8 | [a] | [a] |
| C10 | 36.9 | 36.8 |
| C20/C22 | 37.3 | 37.1 |
| C1 | 37.9 | 37.9 |
| C24 | 39.8 | 39.7 |
| C12 | 40.3 | 40.3 |
| C4 | 42.1 | 42.1 |
| C13 | 42.7 | 42.7 |
| C9 | 50.4 | 50.5 |
| C14/C17 | 57.0/57.3 | 57.1/57.3 |
| C3 | 71.1 | 71.2 |
| C6 | 120.6 | 120.7 |
| C5 | 141.8 | 141.7 |

Spectra were obtained at 310 and 334 K (above and below the $T_m$ of SM).
[a] Not resolved in this phase.

are observed (Fig. 6). Particularly, the $(CH_2)_n$ main chain resonance is shifted to higher ppm and broadens slightly in the cholesterol-containing sample (see Fig. 6C and D). The shift reflects a higher amount of *trans* conformations (more ordered) for the cholesterol containing sample in agreement with previous $^2H$ results on other saturated chain phospholipids above $T_m$ [3,56,58]. The $^{13}C$ chemical shifts of the main chain $(CH_2)_n$ observed in SM and SM/Chol bilayers can be summarized: 32.5, 32.2, 31.5, and 30.5 ppm for SM $L_\beta$, SM/Chol below $T_m$, SM/Chol above $T_m$, and SM $L_\alpha$, respectively. The $^{13}C$ chemical shift to lower ppm with cholesterol and measurements performed below and above $T_m$ in these samples indicates a decrease in order and increase in mobility. The other noticeable difference in the $^{13}C$ spectrum is the significant sharpening of the C3 resonance when cholesterol is present. The C3 resonance has a FWHM = 113, 66, 49, and 37 Hz in SM $L_\beta$, SM $L_\alpha$, SM/Chol above $T_m$, and SM/Chol below $T_m$, respectively. This shows that the sharpening of the C3 resonance is observed regardless of whether the sample is above or below $T_m$ when cholesterol is present (compare Figs. 5A and B and Figs. 6A and B). This indicates that the mobility at this site is increased both above and below $T_m$ when cholesterol is incorporated in the bilayer. An increased mobility for this site below $T_m$ is not particularly surprising since, the fluidity of the bilayer increases and sharpening of the $^{13}C$ resonances is observed at many of the sites in SM/Chol. However, a sharpening of the C3 resonance above $T_m$ is somewhat surprising at first since, the acyl chain becomes more ordered and the bilayer less fluid when cholesterol is present. One explanation for this is that cholesterol disturbs the hydrogen-bonding environment at the C3 hydroxyl group causing a decrease in the rigidity of this site. This hydroxyl group has been postulated to participate in intermolecular and intramolecular hydrogen bonding with neighboring SM molecules at the amide and the oxygen groups of the phosphate, respectively [66]. The potential formation of water bridges between SM molecules has also been discussed [67]. This idea that cholesterol disrupts some of these hydrogen bonding motifs at the SM–water interface is in agreement with some previous X-ray diffraction results where a reduction in the inter-bilayer water thickness was reported [68]. The increased mobility of this site could be a strong indicator that some

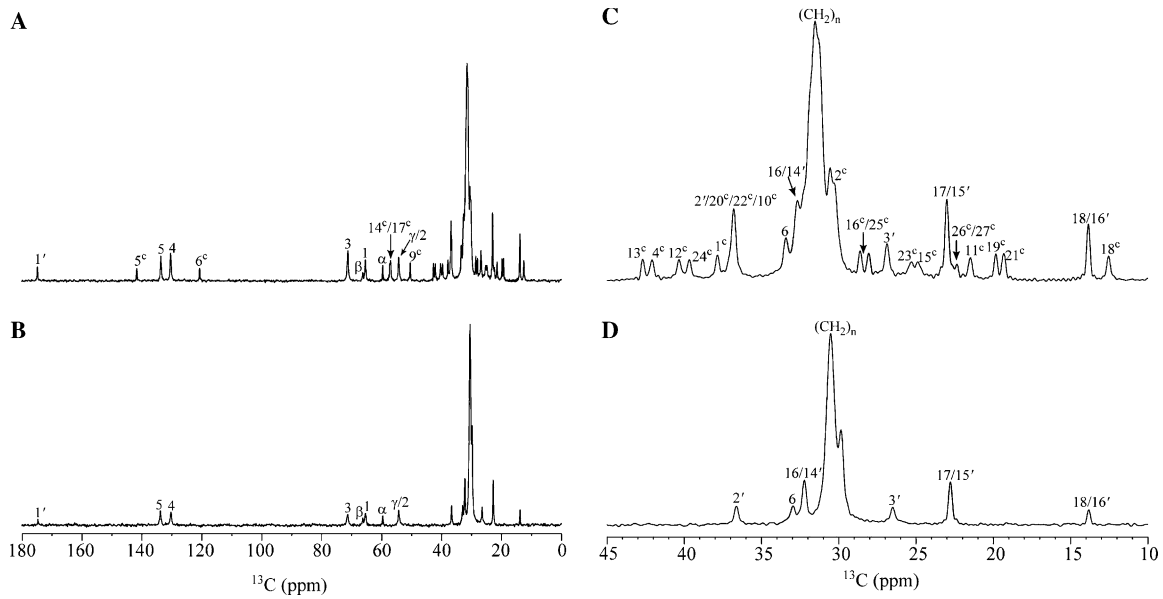


Fig. 6. $^{13}$C CP-MAS NMR spectrum collected with a 2 ms contact time at 334 K (above $T_m$) for (A) SM/Chol and (B) pure SM bilayers. A blow up of the crowded acyl chain region (10–45 ppm) is shown for (C) SM/Chol and (D) SM. The superscript c denotes cholesterol resonances.

of these hydrogen bonding environments at the C3 hydroxyl are disrupted by the incorporation of cholesterol regardless of whether the sample is above or below $T_m$. It should also be noted that when comparing the FWHM of SM/Chol above and below $T_m$, the line width below $T_m$ is sharper. This probably does not indicate a higher degree of mobility below $T_m$ at this site but, rather an increase in sample homogeneity.

### 3.3. Two-dimensional $^1$H–$^{13}$C dipolar HETCOR NMR of SM and SM/Chol bilayers

The 2D $^1$H/$^{13}$C dipolar HETCOR spectra of SM bilayers at 310 and 334 K (in the $L_\beta$ and $L_\alpha$ phases) are presented in Fig. 7. In the $L_\beta$ phase (Fig. 7A), the $^1$H line widths are broad and the resolution is poor while, the $L_\alpha$ phase (Fig. 7B) displays excellent resolution and chemical shift dispersion in both the $^{13}$C and $^1$H dimensions. The 2D HETCOR spectrum collected in the $L_\alpha$ phase was utilized to distinguish and assign the C6 and C16/C14′ $^{13}$C resonances. It was also helpful in assigning the high ppm shoulder in the $^1$H MAS spectrum (Fig. 3) to H3′. Further, the HETCOR spectrum confirms that the $^{13}$C resonance observed at 54.3 ppm is indeed an overlap of both the Cγ and C2 environments as previously proposed [26]. The $^1$H chemical shifts of these two groups are distinct and as a result the single $^{13}$C resonance is separated into two peaks in the $^1$H dimension at the expected $^1$H chemical shifts. It is also interesting to note that the $^1$H correlation peak for the $^{13}$C carbonyl (C1′) resonance is H2′. The carbonyl site has no directly bonded protons and the neighboring protons at C2′ site are responsible for cross polarizing the carbonyl carbon. These results show the advantage of going to multi-dimensional correlation NMR experiments in these complex lipid systems to assist in chemical shift assignment and increase resolution.

The HETCOR spectrum of SM obtained in the $L_\beta$ phase (Fig. 7A) displays broad resonance lines in the $^1$H dimension as a result of the strong $^1$H–$^1$H dipolar interactions that are not completely averaged by the combination of lipid mobility and MAS. Recently, the utilization of FSLG $^1$H homonuclear decoupling in conjunction with $^{13}$C detected dipolar HETCOR experiments has been presented in organic solids and resulted in well resolved resonances in the $^1$H dimension [41]. This experiment was performed and is displayed in Fig. 7C. The $^1$H dimension clearly displays improved line widths compared to the conventional dipolar HETCOR spectrum (see Fig. 7A). The $^1$H line width in the FSLG-HETCOR spectrum is ~430 Hz compared to the line width in the conventional HETCOR experiment ($L_\beta$ phase) where it was ~1.7 kHz measured at the $(CH_2)_n$. This shows that the FSLG technique should be successful in the study of gel phase lipids although, the resolution is not nearly as good as observed in the $L_\alpha$ phase. When comparing the FSLG spectrum with the conventional HETCOR spectrum it should also be noted that the signal-to-noise (S/N) in the FSLG-HETCOR is lower and headgroup resonances 1, 2, and 3 are not observed. This is due to the efficiency of the LG-CP transfer which is lower than the traditional CP transfer implemented in the conventional dipolar HETCOR spectrum shown in Fig. 7A [69]. The breadth of these resonances in both the $^{13}$C and $^1$H dimensions make them difficult to observe. The FSLG technique does not improve the observed $^1$H resolution when applied above $T_m$ in SM or SM/Chol and below $T_m$ in SM/Chol. In the latter case, the chain mobility induced by cholesterol presence approaches the line widths obtained with FSLG and no additional

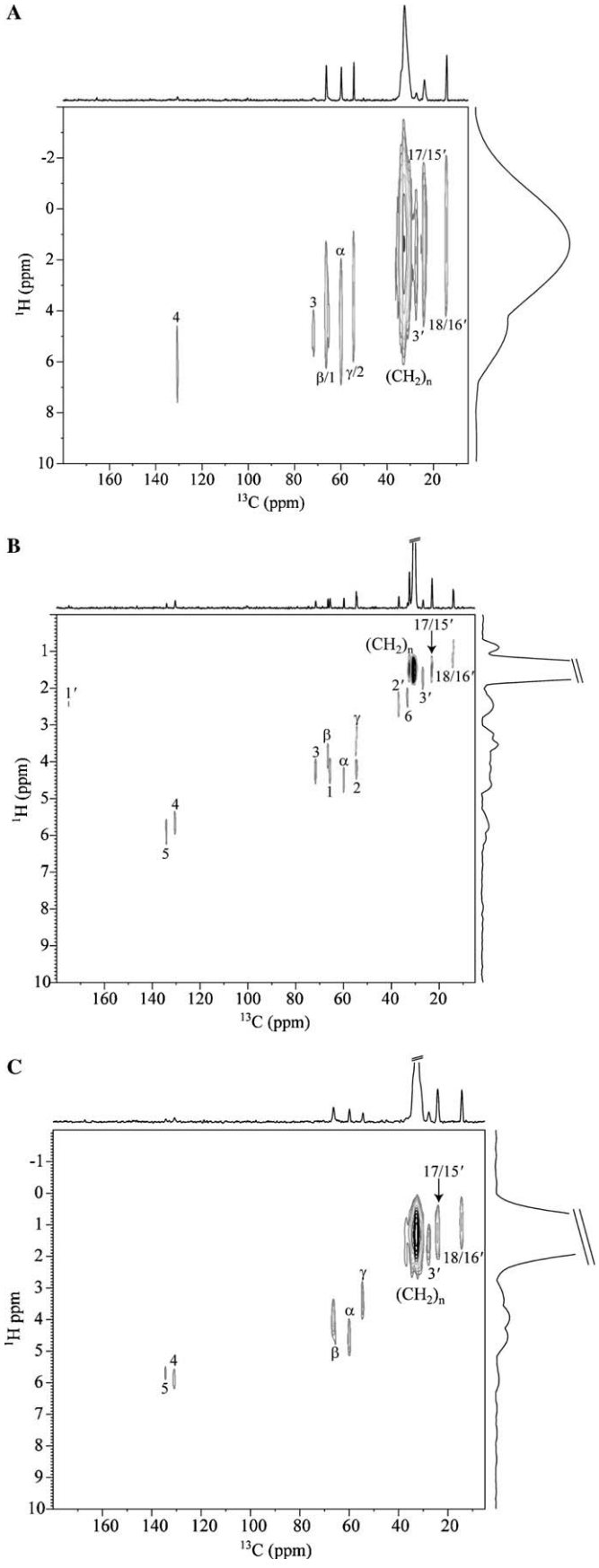


Fig. 7. 2D $^{1}$H/$^{13}$C dipolar HETCOR NMR spectra with 1 ms contact time for SM at (A) 310 K (below $T_m$) and (B) 334 K (above $T_m$). 2D $^{1}$H/$^{13}$C FSLG-HETCOR for (C) SM at 310 K (below $T_m$).

improvement in resolution was observed. This is in agreement with previous results where MREV-8 $^{1}$H homonuclear decoupling did not improve the resolution in 2D dipolar HETCOR spectra of DMPC/Chol bilayers above $T_m$ at similar MAS speeds [38]. The results presented here strongly indicate that $^{1}$H homonuclear decoupling is not a requirement in lipid bilayers below $T_m$ when significant amounts of cholesterol are present, however significant improvement will likely be observed in pure lipids in the gel phase as indicated by the results presented for SM in Fig. 7C.

The 2D dipolar HETCOR spectra for SM/Chol at 310 and 334 K (below and above $T_m$) are depicted Figs. 8A and B, respectively. As discussed above application of FSLG during the $t_1$ evolution period did not improve the resolution in the $^{1}$H dimension thus, the spectra presented here were generated with the conventional 2D dipolar HETCOR technique. Below $T_m$, similar line widths are observed for SM/Chol (Fig. 8A) in comparison to the FSLG experiment on pure SM (Fig. 7C). This is likely the reason why no additional improvement was observed when implementing FSLG. Above $T_m$, line widths close to the ones observed in pure $L_\alpha$ SM are observed (compare to Fig. 7B). All the observed resonances are assignable to SM and cholesterol groups. Above $T_m$ there is a decrease in intensity of the cholesterol resonances compared to the HETCOR spectrum collected below $T_m$ that should be mentioned. Specifically, cholesterol resonances 5$^{c}$ and 6$^{c}$ are not observed. This is attributed to the increased mobility above $T_m$ that decreases the C–H dipolar coupling and hence the CP efficiency. In the 1D $^{13}$C CP-MAS NMR spectrum the loss in S/N above $T_m$ in SM/Chol was not as significant as in the HETCOR spectra. This is attributed to utilization of a longer CP contact time of 2 ms (1 ms in the HETCOR) and a ramped spin-lock pulse in the 1D case. The ramped CP sequence increases the overall S/N [45] and has been shown to be more effective in lipids above $T_m$ than conventional CP [70]. Inclusion of a ramped CP sequence into the HETCOR will likely improve the S/N and overall quality of the 2D spectra.

### 3.4. $^{13}$C cholesterol chemical shifts in SM bilayers

A complete $^{1}$H/$^{13}$C NMR assignment of the cholesterol chemical shifts in $L_\alpha$ DMPC bilayers has recently been reported [37]. The cholesterol resonances observed in this study on SM bilayers were assigned based on that report since they appear at similar chemical shifts (see Table 3). However, there are some subtle differences that should be noted and discussed. The $^{13}$C chemical shift referencing in the previous study was set by assigning the C18 methyl group to 11.84 ppm, the chemical shift observed in the solution NMR spectrum of cholesterol in $CCl_4$. The chemical shift referencing in this study was based on setting the $^{13}$C chemical shift to a secondary standard of glycine. Thus, the chemical shifts reported here are real chemical shifts referenced to TMS. The present results show that

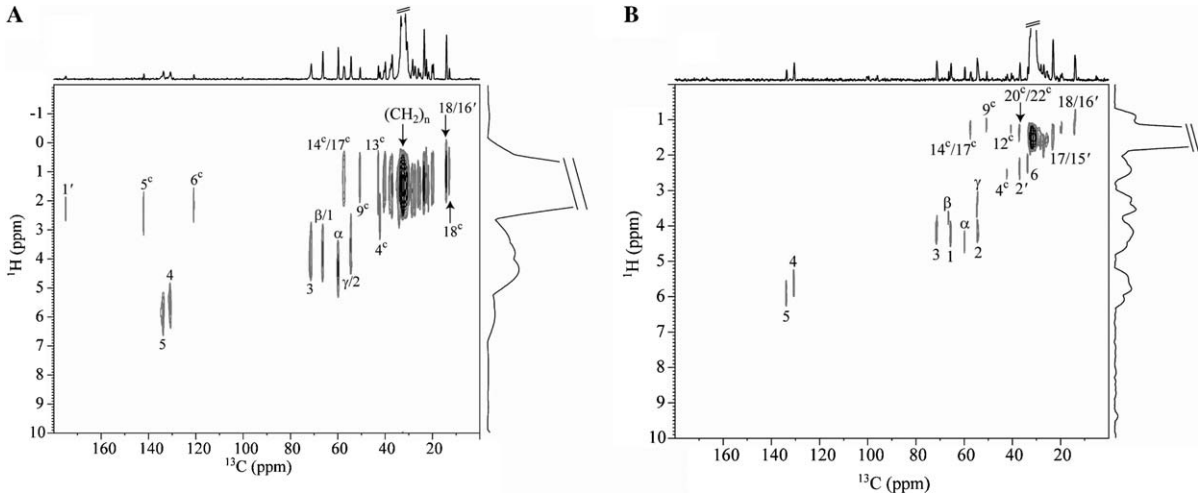


Fig. 8. 2D $^1$H/$^{13}$C dipolar HETCOR NMR spectra with 1 ms contact time for SM/Chol at (A) 310 K (below $T_m$) and (B) 334 K (above $T_m$). The superscript c denotes cholesterol resonances.

the cholesterol shifts in lipid bilayers can differ significantly than those observed in solution NMR studies. For example, the actual chemical shift of the C18 resonance of cholesterol in a SM bilayer below $T_m$ is 12.7 ppm. This chemical shift is 1 ppm downfield with respect to the shift observed in solution NMR where cholesterol is dissolved in $CCl_4$. The cholesterol $^{13}$C chemical shift differences between DMPC/Chol and SM/Chol discussed below accounts for this referencing difference.

The cholesterol $^{13}$C chemical shifts observed in SM/Chol bilayers are within 0.0–0.4 ppm when compared with the shifts observed in DMPC/Chol with the exception that the C5 resonance was 0.7 ppm higher in SM/Chol above $T_m$. The reason for a shift to higher ppm of the C5 resonance in SM/Chol is unknown, but could indicate a difference in how this double bond environment interacts with SM compared to DMPC. A number of the cholesterol $^{13}$C chemical shifts in DMPC/Chol were similar to the ones observed here in SM/Chol. Specifically, the C18, C21, C19, C10, C3 and C6 were essentially identical. This is not surprising for the C18, C21, C19 and C10 environments since these are all methyl resonances and the latter is a quaternary carbon. The observation that the C3 resonance is identical in SM/Chol and DMPC/Chol indicates that the hydrogen bonding interaction at the C3 hydroxyl of cholesterol is probably similar in the two lipids. This is a strong indicator that there is no direct hydrogen bond between the cholesterol hydroxyl group and the lipid interfacial region considering the significant differences between the two lipid backbones (sphingosine in SM and glycerol in DMPC). One explanation for the similarity is that in both systems the hydrogen-bonding partner of the cholesterol C3 hydroxyl is water. It is also interesting to note that the shift of the C6 resonance is identical. The C6 is the other double bond resonance and the fact that it is identical yet the adjacent double bonded C5 is shifted 0.7 ppm downfield in SM/Chol is unknown.

The $^{13}$C chemical shifts of the cholesterol ring carbons display shifts to lower ppm between 0.1 and 0.4 ppm compared to DMPC/Chol. The reason for these variations are unknown however, as quantum chemical shift calculations get better the reason for this variability in different lipid/Chol systems should be determinable [71]. The alkyl tail of cholesterol showed some similarities and some differences. The terminal methyls C26/C27 and the C25 methine group were 0.1 ppm lower than in DMPC/Chol while, C24 was identical and C23 and C22 were 0.1 and 0.3 ppm higher, respectively. Assuming exclusively that differences in the $CH_2$ alkyl groups of cholesterol are due to the amount of *trans*/*gauche* conformers than the higher shifts observed for C23 and C22 carbons can be interpreted to result due to a higher fraction of *trans* conformations and thus a more ordered environment in SM/Chol compared to DMPC/Chol. Further support for this comes from the $^{13}$C spectrum of SM/Chol below $T_m$ where the shifts of the C23 and C22 carbons are to even higher ppm (0.5 ppm higher than in DMPC/Chol). Taken together these results indicate a greater degree of order of the alkyl chain in SM/Chol above $T_m$ compared to DMPC/Chol and that this ordering of cholesterol alkyl chain increases in SM/Chol below $T_m$. If the assumption that the shifts of the $CH_2$ cholesterol alkyl chain are correct and due to changes in the ratio of *trans*/*gauche* conformers then we can conclude that cholesterol ordering is directly correlated with the ordering of the lipid environment and that the two constituents interact cooperatively.

## 4. Conclusions

The present report gives a full $^1$H/$^{13}$C NMR assignment for SM/Chol bilayers. 2D dipolar HETCOR NMR experiments aided in the spectral assignment of SM and allowed an expansion on previous assignments. FSLG-HETCOR was presented on a bilayer lipid system for the first time

and was shown to significantly improve resolution in the gel state while not being a requirement in the $L_\alpha$ phase or in SM/Chol bilayers below $T_m$. The $^1H$ line width and the $^{13}C$ chemical shift of $CH_2$ resonances are sensitive to the ordering and mobility of the SM saturated chain. The cholesterol $^{13}C$ chemical shifts show some significant similarities and differences compared to DMPC/Chol. It was shown that the chemical shift of the cholesterol alkyl tail can be used to measure cholesterol ordering. The cholesterol chemical shift variations observed indicate a higher degree of order in SM/Chol bilayers compared to DMPC/Chol bilayers. Other chemical shift differences indicate that the sterol–lipid interaction in SM is different than in DMPC. The NMR techniques presented herein are broadly applicable to sterol–lipid interactions in the context of understanding the lipid raft phenomenon and should also be powerful methods for the study of protein–lipid interactions.

## References


[1] D.A. Brown, E. London, Structure of detergent-resistant membrane domains: does phase separation occur in biological membranes? Biochem. Biophys. Res. Commun. 240 (1997) 1–7.

[2] D.A. Brown, E. London, Function of lipid rafts in biological membranes, Annu. Rev. Cell Dev. Biol. 14 (1998) 111–136.

[3] M.R. Vist, J.H. Davis, Phase equilibria of cholesterol/dipalmitoylphosphatidylcholine mixtures: $^2H$ nuclear magnetic resonance and differential scanning calorimetry, Biochemistry 29 (1990) 451–464.

[4] S.L. Veatch, I.V. Polozov, K. Gawrisch, S.L. Keller, Organization in lipid membranes containing cholesterol, Phys. Rev. Lett. 89 (2002) 268101.

[5] S.L. Veatch, S.L. Keller, Separation of liquid phases in giant vesicles of ternary mixtures of phospholipids and cholesterol, Biophys. J. 85 (2003) 3074–3083.

[6] S.L. Veatch, I.V. Polozov, K. Gawrisch, S.L. Keller, Liquid domains in vesicles investigated by NMR and fluorescence microscopy, Biophys. J. 86 (2004) 2910.

[7] S.L. Veatch, S.L. Keller, Miscibility phase diagrams of giant vesicles containing sphingomyelin, Phys. Rev. Lett. 94 (2005) 148101.

[8] R.F.M. de Almeida, A. Fedorov, M. Prieto, Sphingomyelin/phosphatidylcholine/cholesterol phase diagram: boundaries and composition of lipid rafts, Biophys. J. 85 (2003) 2406–2416.

[9] C. Dietrich, L.A. Bagatolli, Z.N. Volovyk, N.L. Thompson, M. Levi, K. Jacobson, E. Gratton, Lipid rafts reconstituted in model membranes, Biophys. J. 80 (2001) 1417–1428.

[10] C. Nicolini, P. Thiyagarajan, R. Winter, Small-scale composition fluctuations and microdomain formation in lipid raft models as revealed by small-angle neutron scattering, Phys. Chem. Chem. Phys. 6 (2004) 5531–5534.

[11] H.A. Rinia, M.M.E. Snel, J.P.J.M. van der Eerden, B. de Kruijff, Visualizing detergent resistant domains in model membranes with atomic force microscopy, FEBS Lett. 501 (2001) 92–96.

[12] Y. Barenholz, T.E. Thompson, Sphingomyelins in bilayers and biological membranes, Biochim. Biophys. Acta 604 (1980) 129–158.

[13] R.G.W. Anderson, K. Jacobson, A role for lipid shells in targeting proteins to caveolae, rafts, and other lipid domains, Science 296 (2002) 1821–1825.

[14] R.G. Parton, K. Simons, Digging into caveolae, Science 269 (1995) 1398–1399.

[15] D. Brown, J. Rose, Sorting of GPI-anchored proteins to glycolipid-enriched membrane subdomains during transport to the apical cell surface, Cell 68 (1992) 533–544.

[16] E. Ikonen, Roles of lipid rafts in membrane transport, Curr. Opin. Cell Biol. 13 (2001) 470–477.

[17] B.Y. van Duyl, D. Ganchev, V. Chupin, B. de Kruijff, J.A. Killian, Sphingomyelin is much more effective than saturated phosphatidylcholine in excluding unsaturated phosphatidylcholine from domains formed with cholesterol, FEBS Lett. 547 (2003) 101–106.

[18] J.A. Urbina, S. Pekerar, H. Le, J. Patterson, B. Montez, E. Oldfield, Molecular order and dynamics of phophatidylcholine bilayer membranes in the presence of cholesterol, ergosterol and lanosterol: a comparative study using $^2H$-, $^{13}C$-, and $^{31}P$-NMR spectroscopy, Biochim. Biophys. Acta 1238 (1995) 163–176.

[19] C. Leguerneve, M. Auger, New approach to study fast and slow motions in lipid bilayers: Application to dimyristoylphophatidylcholine-cholesterol interactions, Biophys. J. 68 (1995) 1952–1959.

[20] J. Forbes, C. Husted, E. Oldfield, High-field, high-resolution proton "magic-angle" sample-spinning nuclear magnetic resonance spectroscopic studies of gel and liquid crystalline lipid bilayers and the effects of cholesterol, J. Am. Chem. Soc. 110 (1988) 1059–1065.

[21] W. Guo, J.A. Hamilton, A multinuclear solid-state NMR study of phospholipid–cholesterol interactions. Dipalmitoylphosphatidylcholine–cholesterol binary system, Biochemistry 34 (1995) 14174–14184.

[22] D.E. Warschawski, P.F. Devaux, $^1H$–$^{13}C$ polarization transfer in membranes: a tool for probing lipid dynamics and the effect of cholesterol, J. Magn. Reson. 177 (2005) 166–171.

[23] J. Forbes, J. Bowers, X. Shan, L. Moran, E. Oldfield, M.A. Moscarello, Some new developments in solid-state nuclear magnetic resonance spectroscopic studies of lipids and biological membranes, including the effects of cholesterol in model and natural systems, J. Chem. Soc., Faraday Trans. I. 84 (1988) 3821–3849.

[24] W. Guo, J.A. Hamilton, C-13 MAS NMR studies of crystalline cholesterol and lipid mixtures modeling atherosclerotic plaques, Biophys. J. 71 (1996) 2857–2868.

[25] R.M. Epand, R.F. Epand, A.D. Bain, B.G. Sayer, D.W. Hughes, Properties of polyunsaturated phosphatidylcholine membranes in the presence and absence of cholesterol, Magn. Reson. Chem. 42 (2004) 139–147.

[26] K.S. Bruzik, B. Sobon, G.M. Salamonczyk, Nuclear magnetic resonance study of sphingomyelin bilayers, Biochemistry 29 (1990) 4017–4021.

[27] L.-M. Chi, C.-H. Hsieh, W.-G. Wu, Probing the double bond and phase properties of natural lipid dispersions by cross polarization/magic angle spinning $^{13}C$ NMR, J. Chin. Chem. Soc. 39 (1992) 35–42.

[28] W. Guo, V. Kurze, T. Huber, N.H. Afdhal, K. Beyer, J.A. Hamilton, A solid-state NMR study of phospholipid–cholesterol interactions: sphingomyelin–cholesterol binary systems, Biophys. J. 83 (2002) 1465–1478.

[29] R.M. Epand, R.F. Epand, Non-raft forming sphingomyelin–cholesterol mixtures, Chem. Phys. Lipids 132 (2004) 37–46.

[30] R.M. Epand, Cholesterol in bilayers of sphingomyelin or dihydrosphingomyelin at concentrations found in ocular lens membranes, Biophys. J. 84 (2003) 3102–3110.

[31] J.-Z. Chen, R.E. Stark, Evaluating spin diffusion in MAS-NOESY spectra of phopholipid multibilayers, Solid State Nucl. Magn. Reson. 7 (1996) 239–246.

[32] D. Huster, K. Arnold, K. Gawrisch, Investigation of lipid organization in biological membranes by two-dimensional nuclear overhauser enhancement spectroscopy, J. Phys. Chem. B 103 (1999) 243–251.

[33] D. Huster, K. Gawrisch, NOESY NMR crosspeaks between lipid headgroups and hydrocarbon chains: spin diffusion or molecular disorder, J. Am. Chem. Soc. 121 (1999) 1992–1993.

[34] D.E. Warschawski, P. Fellmann, P.F. Devaux, High-resolution $^{31}P$–$^1H$ two-dimensional nuclear magnetic resonance spectra of unsonicated lipid mixtures spinning at the magic-angle, Eur. Biophys. J. 25 (1996) 131–137.

[35] M. Hong, K. Schmidt-Rohr, D. Nanz, Study of phospholipid structure by $^1H$, $^{13}C$, and $^{31}P$ dipolar couplings from two-dimensional NMR, Biophys. J. 69 (1995) 1939–1950.

[36] C.W.B. Lee, R.G. Griffin, Two-dimensional $^{1}H/^{13}C$ heteronuclear chemical shift correlation spectroscopy of lipid bilayers, Biophys. J. 55 (1989) 355–358.
[37] O. Soubias, F. Jolibois, V. Réat, A. Milon, Understanding sterol–membrane interactions, part II: Complete $^{1}H$ and $^{13}C$ assignments by solid-state NMR spectroscopy and determination of the hydrogen-bonding partners of cholesterol in a lipid bilayer, Chem. Eur. J. 10 (2004) 6005–6014.
[38] O. Soubias, V. Réat, O. Saurel, A. Milon, High resolution 2D $^{1}H$–$^{13}C$ correlation of cholesterol in model membranes, J. Magn. Reson. 158 (2002) 143–148.
[39] O. Soubias, M. Piotto, O. Saurel, O. Assemat, V. Réat, A. Milon, Detection of natural abundance $^{1}H$–$^{13}C$ correlations of cholesterol in its membrane environment using a gradient enhanced HSQC experiment under high resolution magic angle spinning, J. Magn. Reson. 165 (2003) 303–308.
[40] M. Lee, W.I. Goldburg, Nuclear-magnetic-resonance line narrowing by a rotating rf field, Phys. Rev. A 140 (1965) 1261–1271.
[41] B.-J. van Rossum, H. Förster, H.J.M. de Groot, High-field and high-speed CP-MAS $^{13}C$ NMR heteronuclear dipolar-correlation spectroscopy of solids with frequency-switched Lee–Goldburg homonuclear decoupling, J. Magn. Reson. 124 (1997) 516–519.
[42] A. Ramamoorthy, C.H. Wu, S.J. Opella, Three-dimensional solid-state nmr experiment that correlates the chemical shift and dipolar coupling frequencies of two heteronuclei, J. Magn. Reson. B 107 (1995) 88–90.
[43] A. Ramamoorthy, C.H. Wu, S.J. Opella, Experimental aspects of multidimensional solid-state NMR correlation spectroscopy, J. Magn. Reson. 140 (1999) 131–140.
[44] C.H. Wu, A. Ramamoorthy, L.M. Gierasch, Simultaneous characterization of the amide $^{1}H$ chemical shift, $^{1}H$–$^{15}N$ dipolar, and $^{15}N$ chemical shift interaction tensors in a peptide bond by three-dimensional solid-state NMR spectroscopy, J. Am. Chem. Soc. 117 (1995) 6148–6149.
[45] G. Metz, X.L. Wu, S.O. Smith, Ramped-amplitude cross polarization in magic-angle-spinning NMR, J. Magn. Reson. A 110 (1994) 219–227.
[46] K. Schmidt-Rohr, J. Clauss, H.W. Spiess, Correlation of structure, mobility, and morphological information in heterogeneous polymer materials by two-dimensional wideline-separation NMR spectroscopy, Macrmolecules 25 (1992) 3273–3277.
[47] B.-J. van Rossum, G.J. Boender, High magnetic field for enhanced proton resolution in high-speed CP/MAS heteronuclear $^{1}H$–$^{13}C$ dipolar correlation spectroscopy, J. Magn. Reson. A 120 (1996) 274–277.
[48] B.-J. van Rossum, C.P. de Groot, V. Ladizhansky, S. Vega, H.J.M. de Groot, A method for measuring heteronuclear ($^{1}H$–$^{13}C$) distances in high speed MAS NMR, J. Am. Chem. Soc. 122 (2000) 3465–3472.
[49] M. Mehring, J.S. Waugh, Magic-angle NMR experiments in solids, Phys. Rev. B 5 (1972) 3459–3472.
[50] A.E. Bennett, C.M. Rienstra, M. Auger, K.V. Lakshmi, R.G. Griffin, Heteronuclear decoupling in rotating solids, J. Chem. Phys. 103 (1995) 6951–6958.
[51] S.V. Dvinskikh, V. Castro, D. Sandström, Heating caused by radio frequency irradiation and sample rotation in $^{13}C$ magic angle spinning NMR studies of lipid membranes, Magn. Reson. Chem. 42 (2004) 875–881.
[52] K. Gawrisch, V.E. Nadukkudy, I.V. Polozov, Novel NMR tools to study structure and dynamics of biomembranes, Chem. Phys. Lipids 116 (2002) 135–151.
[53] K.S. Bruzik, Synthesis and spectral properties of chemically and stereochemically homogeneous sphingomyelin and its analogues, J. Chem. Soc., Perkin Trans. I. (1988) 423–431.
[54] D. Massiot, F. Fayon, M. Capron, I. King, S. LeCalvé, B. Alonso, J.-O. Durand, B. Bujoli, Z. Gan, G. Hoatson, Modelling one- and two-dimensional solid-state NMR spectra, Magn. Reson. Chem. 40 (2002) 70–76.
[55] Y. Barenholz, J. Suurkuusk, D. Mountcastle, T.E. Thompson, R.L. Biltonen, A calorimetric study of the thermotropic phase behavior of aqueous dispersions of natural and synthetic sphingomyelins, Biochemistry 15 (1976) 2441–2447.
[56] E. Oldfield, D. Chapman, W. Derbyshire, Deuteron resonance: a novel approach to the study of hydrocarbon chain mobility in membrane systems, FEBS Lett. 16 (1971) 102–104.
[57] M.F. Brown, J. Seelig, Influence of cholesterol on the polar region of phosphatidylcholine and phosphatidylethanolamine bilayers, Biochemistry 17 (1978) 381–384.
[58] J.H. Davis, The description of membrane lipid conformation, order and dynamics by $^{2}H$-NMR, Biochim. Biophys. Acta 737 (1983) 117–171.
[59] G.P. Holland, S.K. McIntyre, T.M. Alam, Distinguishing Individual Lipid Headgroup Mobility and Phase Transitions in Raft-Forming Lipid Mixtures with $^{31}P$ MAS NMR, Biophys. J. 90 (2006) 4248–4260.
[60] J.F. Nagle, Y. Liu, S. Tristram-Nagle, R.M. Epand, R.E. Stark, Re-analysis of magic angle spinning nuclear magnetic resonance determination of interlamellar waters in lipid bilayer dispersions, Biophys. J. 77 (1999) 2062–2065.
[61] T.J. McIntosh, S.A. Simon, D. Needham, C.-H. Huang, Structure and cohesive properties of sphingomyelin/cholesterol bilayers, Biochemistry 31 (1992) 2012–2020.
[62] E. Oldfield, D. Chapman, Effects of cholesterol and cholesterol derivatives on hydrocarbon chain mobility in lipids, Biochem. Biophys. Res. Commun. 43 (1971) 610–616.
[63] E. Oldfield, D. Chapman, Molecular dynamics of cerebroside–cholesterol and sphingomyelin–cholesterol interactions: implications for myelin membrane structure, FEBS Lett. 21 (1972) 303–306.
[64] P.R. Cullis, M.J. Hope, The bilayer stabilizing role of sphingomyelin in the presence of cholesterol: a $^{31}P$ NMR study, Biochim. Biophys. Acta 597 (1980) 533–542.
[65] W. Guo, J.A. Hamilton, A multinuclear solid-state NMR study of phospholipid–cholesterol interactions. Dipalmitoylphosphatidylcholine–cholesterol binary system, Biochemistry 34 (1995) 14174–14184.
[66] P. Niemelä, M.T. Hyvönen, I. Vattulainen, Structure and dynamics of sphingomyelin bilayer: insight gained through systematic comparison to phosphatidylcholine, Biophys. J. 87 (2004) 2976–2989.
[67] C.M. Talbott, I. Vorobyov, D. Borchman, K.G. Taylor, D.B. DuPré, M.C. Yappert, Conformational studies of sphingolipids by NMR spectroscopy. II. Sphingomyelin, Biochim. Biophys. Acta 1467 (2000) 326–337.
[68] P.R. Maulik, G.G. Shipley, N-Palmitoyl sphingomyelin bilayers: structure and interactions with cholesterol and dipamitoylphosphatidylcholine, Biochemistry 35 (1996) 8025–8034.
[69] V. Ladizhansky, S. Vega, Polarization transfer dynamics in Lee–Goldburg cross polarization nuclear magnetic resonance experiments on rotating solids, J. Chem. Phys. 112 (2000) 7158–7168.
[70] D.E. Warschawski, P.F. Devaux, Polarization transfer in lipid membranes, J. Magn. Reson. 145 (2000) 367–372.
[71] F. Jolibois, O. Soubias, V. Réat, A. Milon, Understanding sterol–membrane interactions part I: Hartree-Fock versus DFT calculations of $^{13}C$ and $^{1}H$ NMR isotropic chemical shifts of sterols in solution and analysis of hydrogen-bonding effects, Chem. Eur. J. 10 (2004) 5996–6004.